Chemistry–A European Journal
Research Article
doi.org/10.1002/chem.202200669
Chemistry Europe
European Chemical Societies Publishing
www.chemeurj.org

Halogenation of the Hexaphosphabenzene Complex $[(Cp^*Mo)_2(\mu,\eta^6{:}\eta^6\text{-}P_6)]$: Snapshots on the Reaction Progress

Anna Garbagnati,[a] Michael Seidl,[a] Gábor Balázs,[a] and Manfred Scheer*[a]

Abstract: The oxidation of $[(Cp^*Mo)_2(\mu,\eta^6{:}\eta^6\text{-}P_6)]$ (**1**) with halogens or halogen sources was investigated. The iodination afforded the ionic complexes $[(Cp^*Mo)_2(\mu,\eta^3{:}\eta^3\text{-}P_3)(\mu,\eta^1{:}\eta^1{:}\eta^1{:}\eta^1\text{-}P_3I_3)][X]$ ($X = I_3^-$, I^-) (**2**) and $[(Cp^*Mo)_2(\mu,\eta^4{:}\eta^4\text{-}P_4)(\mu\text{-}PI_2)][I_3]$ (**3**), while the reaction with PBr_5 led to the complexes $[(Cp^*Mo)_2(\mu,\eta^3{:}\eta^3\text{-}P_3)(\mu\text{-}Br)_2][Cp^*MoBr_4]$ (**4**) $[(Cp^*MoBr)_2(\mu,\eta^3{:}\eta^3\text{-}P_3)(\mu,\eta^1\text{-}P_2Br_3)]$ (**5**) and $[(Cp^*Mo)_2(\mu\text{-}PBr_2)(\mu\text{-}PHBr)(\mu\text{-}Br)_2]$ (**6**). The reaction of **1** with the far stronger oxidizing agent PCl_5 was followed via time- and temperature-dependent $^{31}P\{^1H\}$ NMR spectroscopy. One of the first intermediates detected at 193 K was $[(Cp^*Mo)_2(\mu,\eta^3{:}\eta^3\text{-}P_3)(\mu\text{-}PCl_2)_2][PCl_6]$ (**8**) which rearranges upon warming to $[(Cp^*Mo)_2(\mu\text{-}PCl_2)_2(\mu\text{-}Cl)_2]$ (**9**), $[(Cp^*MoCl)_2(\mu,\eta^3{:}\eta^3\text{-}P_3)(\mu\text{-}PCl_2)]$ (**10**) and $[(Cp^*Mo)_2(\mu,\eta^4{:}\eta^4\text{-}P_4)(\mu\text{-}PCl_2)][Cp^*MoCl_4]$ (**11**), which could be isolated at room temperature. All complexes were characterized by single-crystal X-ray diffraction, NMR spectroscopy and their electronic structures were elucidated by DFT calculations.

Introduction

The halogenation of white phosphorus is the first step on an industrial scale to transform P_4 to organophosphorus derivatives. First publications on the halogenation of white phosphorus date back more than 120 years.[1,2] In 1940, Wyllie et al. proved that the reaction of P_4 with I_2 leads to P_2I_4 or PI_3, depending on the used stoichiometry, while the reaction of P_4 with Br_2 leads to PBr_3.[3] Based on these results, in 1994, Tattershall et al. reported four series of compounds resulting from the reaction of P_4 with I_2, Br_2 or ICl that were identified by NMR spectroscopy.[4] Later on, Stoppioni et al. presented the first example of a halogenation of coordinated white phosphorus in the coordination sphere of a transition metal by iodine, which resulted in the monocation $[\{CpRu(PPh_3)_2\}_2(\mu,\eta^1{:}\eta^1\text{-}P_4H_2I)]^+$).[5] In 2019, Peruzzini et al. reported the ruthenium-mediated halogenation of white phosphorus, resulting in the complex $[Cp^*Ru(PCy_3)(\mu,\eta^2{:}\eta^4\text{-}P_4Cl_2)RuCp^*]$ bearing the unprecedented P_4Cl_2 moiety.[6] Recently, the stepwise degradation of white phosphorus coordinated to a Ru(II) complex upon the reaction with iodine was postulated by DFT computations.[7] The key role of the metal was demonstrated since the proposed mechanism differs significantly from the concerted one that is valid for uncoordinated white phosphorus.[8] As an alternative access, P_4 moieties already converted to polyphosphorus complexes might be a valuable approach to functionalized polyphosphorus complexes.

Our recent study on the iodination of the *cyclo*-E_5 complexes $[Cp^*M(\eta^5\text{-}E_5)]$ (M = Fe, Ru; E = P, As)[9] has shown that this is a powerful method for the high-yield synthesis of new types of functionalized polypnictogen compounds (Scheme 1b, red arrow). By examining different halogen sources, the halogenation of the tetrahedrane compound $[\{CpMo(CO)_2\}_2(\mu,\eta^2{:}\eta^2\text{-}P_2)]$ proved to lead to very diverse reaction products (Scheme 1a, red arrow).[10]

These studies clearly show the different reactivities of polyphosphorus complexes with oxidants such as halogens towards an alternative one-electron oxidation. Thus, the oxidation of $[\{CpMo(CO)_2\}_2(\mu,\eta^2{:}\eta^2\text{-}P_2)]$ leads selectively to the dicationic complex $[\{CpMo(CO)_2\}_4(\mu,\eta^2{:}\eta^2{:}\eta^2{:}\eta^2\text{-}P_4)]^{2+}$[11] (Scheme 1a, **B**), while the halogenation yields, depending on the used stoichiometry and halogen, **C**–**E** (Scheme 1a). Similarly, a substantial difference in the one-electron oxidation of $[Cp^*Fe(\eta^5\text{-}P_5)]$ and its oxidation with halogens was realized. While the oxidation leads to the dicationic complex $[(Cp^*Fe)_2(\mu,\eta^{5:5}\text{-}P_{10})]^{2+}$ (Scheme 1b, **G**),[12] the reaction with I_2 yields the nortricylane derivative **H** (Scheme 1b).[9] Since in triple-decker complexes the middle deck is stabilized by two metal fragments, a higher stability of the products in the reaction with halogens is expected, possibly enabling the identification of intermediates and their isolation along the reaction pathway.

Therefore, the redox-active compound $[(Cp^*Mo)_2(\mu,\eta^6{:}\eta^6\text{-}P_6)]$ (**1**)[13] was chosen for a detailed study of its halogenation. The cyclo-voltammogram of this 28 VE complex reveals a reversible one-electron oxidation in which a 27 VE product results in a distorted *cyclo*-P_6 ligand in a bis-allylic arrangement (Scheme 1c, **I**).[14] Herein we report on the oxidation of the hexaphosphabenzene complex $[(Cp^*Mo)_2(\mu,\eta^6{:}\eta^6\text{-}P_6)]$ (**1**) by halogens and

[a] A. Garbagnati, Dr. M. Seidl, Dr. G. Balázs, Prof. Dr. M. Scheer
Institute of Inorganic Chemistry
University of Regensburg
93040 Regensburg (Germany)
E-mail: manfred.scheer@chemie.uni-regensburg.de
Homepage: https://www.uni-regensburg.de/chemie-pharmazie/anorganische-chemie-scheer

Supporting information for this article is available on the WWW under https://doi.org/10.1002/chem.202200669

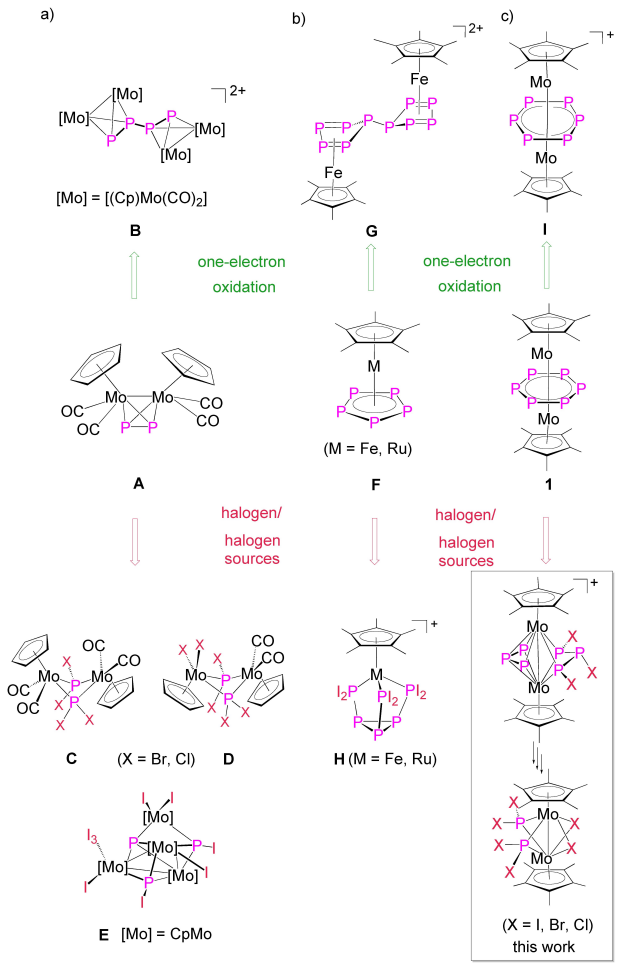

Scheme 1. Selected examples of one-electron oxidations *versus* halogenation reactions of P_n-ligand complexes. Selected P_n ligand complexes are a) the tetrahedrane $[\{CpMo(CO)_2\}_2(\mu,\eta^2{:}\eta^2\text{-}P_2)]$; b) $[Cp^*M(\eta^5\text{-}E_5)]$ (M = Fe, Ru; E = P, As); c) $[(Cp^*Mo)_2(\mu,\eta^6{:}\eta^6\text{-}P_6)]$.

halogen sources such as I_2, PBr_5 and PCl_5 as a novel synthetic approach to unprecedented halogen-functionalized complexes of the type $[(Cp^*Mo)_2P_nX_m]^{+/0}$ (n, m = 1, 2, 3; X = I, Br, Cl) revealing P_nX_m middle decks.

Results and Discussion

The reaction of **1** with an excess of iodine (6 equiv.) in CH_2Cl_2, followed by the layering of the reaction solution with *n*-pentane, leads to $[(Cp^*Mo)_2(\mu,\eta^3{:}\eta^3\text{-}P_3)(\mu,\eta^1{:}\eta^1{:}\eta^1{:}\eta^1\text{-}P_3I_3)][I_3]$ (**2-I$_3$**) as a red crystalline compound in 54% isolated yield (Scheme 2). When a stoichiometric amount of I_2 was used (3 equiv.), a few crystals of the similar complex **2-I** in which I_3^- is replaced by I^- as counterion were isolated, together with $[(Cp^*Mo)_2(\mu,\eta^4{:}\eta^4\text{-}P_4)(\mu\text{-}PI_2)][I_3]$ (**3**) as black blocks in a crystalline yield of 2% (Scheme 2, cf. Supporting Information). The ESI-MS spectrum of the latter reaction solution shows the molecular ion peak of **2** and **3**, together with the one of the paramagnetic complex $[(Cp^*Mo)_2(\mu\text{-}I)_4][I_3]$. The latter compound was already described by *Poli et al.*[15] Possible other products as for instance PI_3 or P_2I_4 could not be detected in the $^{31}P\{^1H\}$ NMR spectrum of the reaction solution which shows only the signals of **2** (see below). The formation of **3** could not be ascertained by ^{31}P NMR spectroscopy due it is paramagnetic nature. Since no signals of the starting material were detected, its full conversion can be assumed. The variable temperature (VT) $^{31}P\{^1H\}$ NMR spectrum of this reaction solution recorded from −80 °C to room temperature shows that the formation of **2** starts already at low temperatures, with **2** being the only P-containing diamagnetic product that could be detected. The spectra at higher temperatures are silent because **2** precipitates completely from the solution already at low temperatures (cf. SI for VT-$^{31}P\{^1H\}$ NMR) and the remaining products are paramagnetic.

Our study of the halogenation of $[\{CpMo(CO)_2\}_2(\mu,\eta^2{:}\eta^2\text{-}P_2)]$ showed that the nature of the halogen (I_2 vs. Br_2) plays a decisive role regarding the type of the resulting compounds.[10] Hence, the reaction of $[(Cp^*Mo)_2(\mu,\eta^6{:}\eta^6\text{-}P_6)]$ (**1**) with PBr_5 as a bromine source was carried out. Due to the higher reactivity of bromine (as compared to iodine), the reaction of **1** with an excess of PBr_5 (6 equiv.) in CH_2Cl_2 was carried out at −40 °C and the reaction solution was slowly warmed up to −20 °C. Precipitation of the concentrated reaction solution with cold *n*-pentane led to a green precipitate which was dissolved in THF and layered with toluene affording a few crystals of $[(Cp^*Mo)_2(\mu,\eta^3{:}\eta^3\text{-}P_3)(\mu\text{-}Br)_2][Cp^*MoBr_4]$ (**4**) (2% yield). The supernatant mother liquor was decanted off and, while warming up to room temperature, crystals of the neutral species $[(Cp^*MoBr)_2(\mu,\eta^3{:}\eta^3\text{-}P_3)(\mu\text{-}P_2Br_3)]$ (**5**) were formed in 17% yield. Performing the reaction under the same conditions but evaporating all volatiles at −10 °C, washing the residue with *n*-pentane and toluene and finally recrystallizing from a mixture of CH_2Cl_2/*n*-pentane, crystals of $[(Cp^*Mo)_2(\mu\text{-}PBr_2)(\mu\text{-}PHBr)(\mu\text{-}Br)_2]$ (**6**) could be isolated (9% yield; Scheme 2). Additionally, also a few crystals of the known side product $[(Cp^*MoBr_2)_2(\mu\text{-}Br)_2]$[16] were formed. The $^{31}P\{^1H\}$ NMR spectrum of the reaction solution shows, among the signals corresponding to **4**[17] and **6**, a broad singlet at 230 ppm corresponding to PBr_3 which overlaps with one of the two signals of **6**. Signals corresponding to **5** could not be detected in the ^{31}P NMR spectrum of the freshly prepared reaction solution, but were only detected after storing the sample at room temperature for five days. This indicates that **5** is not an initial product of the reaction of **1** with PBr_5. Preparing an NMR sample by mixing a precooled solution of **1** and PBr_5 and performing a VT $^{31}P\{^1H\}$ NMR experiment (starting at −80 °C) shows the formation of a very complex reaction mixture (cf. SI) from which no known complexes could be identified. By warming to room temperature, signals corresponding to **6** could be detected. Since the signal of PBr_3 is always detected when using PBr_5 as a reagent, the question arises which part of it results from the halogenation of **1**. ^{31}P NMR spectroscopic investigations showed that only about 30% of the PBr_3 originates from PBr_5 while the remaining 70% follows from the bromination of **1** (see Supporting Information).

Against the background that the reaction of **1** towards a bromine source was predictably more complex than the one with iodine, the question arises as to what would be the

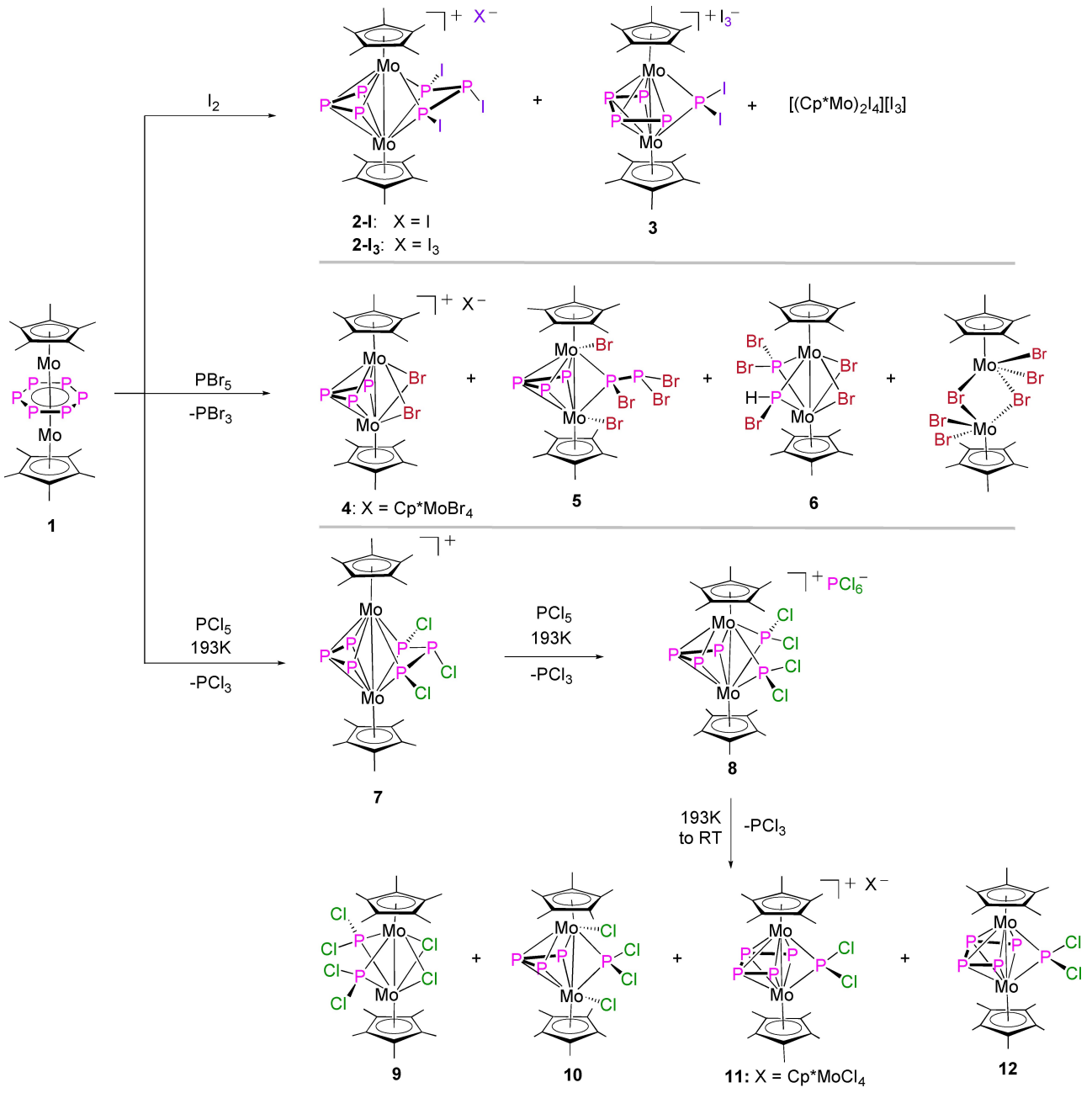

Scheme 2. Reaction of $[(Cp^*Mo)_2(\mu,\eta^6{:}\eta^6\text{-}P_6)]$ with I_2, PBr_5 and PCl_5.

difference in the reactivity towards an even stronger halogenating agent as for instance chlorine. Therefore, a time-dependent $^{31}P\{^1H\}$ NMR study of the reaction of **1** with an excess of PCl_5 (6 equiv.) was carried out at 193 K (Figure 1a). The signal of **1** could not be detected, which proves that its conversion is complete already at 193 K after fifteen minutes. The first $^{31}P\{^1H\}$ NMR spectrum (t_1 = 15 minutes) shows four resonances centered at $\delta = 420.8$, 329.3, 145.1 and −361.7 ppm in a 1:2:2:1 integral ratio, corresponding to an AMM'OO'X spin system (Figure 1a,b) which can be assigned to **7**, based on its similarity with **2** (see below). In addition, a singlet corresponding to PCl_3 ($\delta = 220.0$ ppm) and a singlet at 6.5 ppm which could not be assigned were detected. **7** could not be isolated due to its high instability. Attempts to crystallize it led to the isolation of $[(Cp^*Mo)_2(\mu,\eta^3{:}\eta^3\text{-}P_3)(\mu\text{-}PCl_2)_2][PCl_6]$ (**8**) instead (74% yield, scheme 2). Based on the ^{31}P NMR spectroscopic data, the first product of the reaction of **1** with PCl_5 is **7** which then converts to **8**, where its signals start to appear in the time-dependent NMR study after one hour (t_2 = 1 h; figure 1a). Solutions of **8** in CH_2Cl_2 at room temperature are stable for less than one hour, afterwards the color of the solution starts to change from bright red to dark brown. Its decomposition was monitored by NMR spectroscopy (see Supporting Information). The $^{31}P\{^1H\}$ NMR spectrum of the crystals of **8** dissolved in

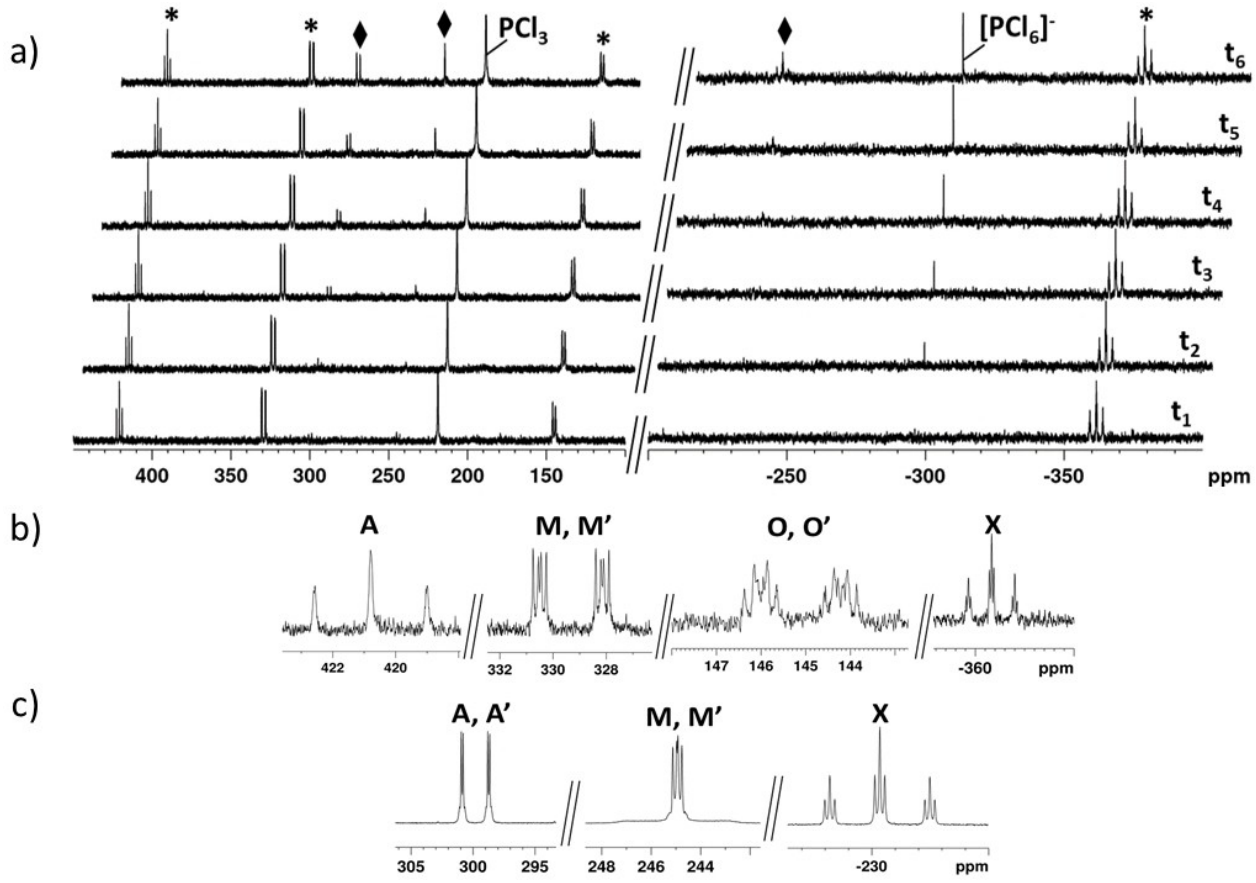

Figure 1. a) Time-dependent $^{31}P\{^1H\}$ NMR spectra of the reaction solution of **1** with PCl_5 at 193 K. * = **7**, ♦ = **8**; **b)** Selected signals of the $^{31}P\{^1H\}$ NMR spectrum of **7** (CD_2Cl_2, 193 K) **c)** Selected signals of the $^{31}P\{^1H\}$ NMR spectrum of **8** (CD_2Cl_2, 233 K).

CD_2Cl_2 at room temperature reveals after seven hours its complete decomposition and formation of $[(Cp^*Mo)_2(\mu\text{-}PCl_2)_2(\mu\text{-}Cl)_2]$ (**9**), $[(Cp^*MoCl)_2(\mu,\eta^3{:}\eta^3\text{-}P_3)(\mu\text{-}PCl_2)]$ (**10**) and PCl_3 (Figure 2).

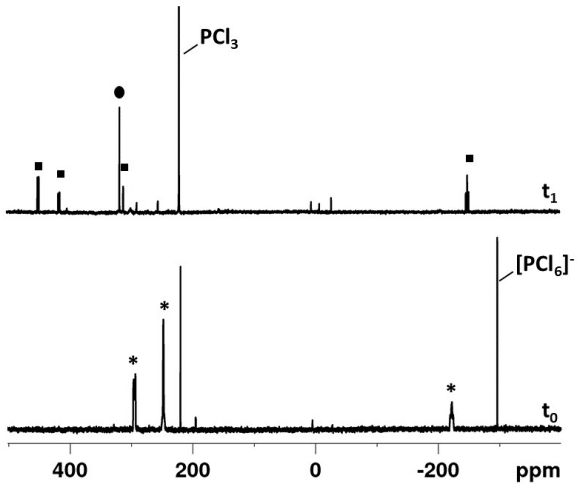

Figure 2. $^{31}P\{^1H\}$ NMR spectra of **8** at $t_0 = 20$ minutes and $t_1 = 7$ h (CD_2Cl_2, 300 K). Whereas, after 20 minutes, only signals of **8** (*) and PCl_3 are visible, after 7 h, its complete decomposition into **9** (●) and **10** (■) is detected.

Moreover, the intensity of the signal corresponding to PCl_3 (220.2 ppm) increases with the temperature, while the one of $[PCl_6]^-$ decreases until it disappears completely at room temperature (cf. SI for VT $^{31}P\{^1H\}$ NMR). By performing the reaction of **1** with PCl_5 directly at room temperature, **9** and **10** can be isolated in 3% and 4% crystalline yield, respectively (Scheme 2). The $^{31}P\{^1H\}$ NMR spectrum of the reaction solution at 25 °C shows the characteristic signals of **9** ($\delta = 317.2$ ppm), **10** (see below) and PCl_3 ($\delta = 220.2$ ppm) among other signals that could not be assigned (cf. SI). Roughly 78% of the PCl_3 originates from **1**, which reflects the low yields of **9** and **10**.[18] Attempts to isolate other products of the chlorination led to the isolation of the 30 VE cationic triple-decker compound $[(Cp^*Mo)_2(\mu,\eta^4{:}\eta^4\text{-}P_4)(\mu\text{-}PCl_2)][Cp^*MoCl_4]$ (**11**) (Scheme 2).

11 is well soluble in CD_2Cl_2 but paramagnetic (cf. Supporting Information) and therefore could not be detected by NMR spectroscopy, but was identified by single crystal X-ray diffraction analysis. In the ^1H NMR spectrum of **11**, the signal of the anion $[Cp^*MoCl_4]^-$ in **11** could be detected at −13.9 ppm as a broad singlet ($\omega_{1/2} = 170$ Hz), which is in line with the reported chemical shift.[19] When **1** was reacted with three equiv. of PCl_5, the neutral analogue of **11**, i.e. $[(Cp^*Mo)_2(\mu,\eta^4{:}\eta^4\text{-}P_4)(\mu\text{-}PCl_2)]$ (**12**), could be isolated in 10% yield.[20] The 31VE triple-decker complex **12** is paramagnetic, but no signals could

be detected by EPR spectroscopy, probably due to its triplet spin state. Crystals of **11** were alternatively obtained by layering a solution of **8** with *n*-pentane in CH_2Cl_2 at room temperature after few days. Therefore, together with **9** and **10**, **11** represents another conversion product of **8** (Scheme 2). Additional proof of this is provided by the ^{1}H NMR spectrum of crystals of **8** dissolved in CD_2Cl_2 which also shows, after 15 days at room temperature, the broad singlet of the counterion of **11**, $[Cp^*MoCl_4]^-$(cf. Supporting Information).[21]

The ^{31}P NMR spectra of **2** and **7** are very similar, both of them showing an AMM'OO'X spin system (cf. Supporting Information). The central phosphorus atom of the allylic-like P_3 unit (P^X) resonates at high field (−327 ppm for **2** and −362 ppm for **7**), while the peripheral P atoms (P^M/$P^{M'}$) resonate at lower field (349 ppm for **2** and 382 ppm for **7**) and show the largest $^1J_{PP}$ coupling constant (~380 Hz). Similar chemical shifts and coupling constants were found for the allylic-like P_3 unit in the complexes **5**, **10** and **8** (for details see Supporting Information), although **5** shows an ADHKX spin system (Figure 3, top) due to the chemically inequivalent peripheral P atoms of the allylic-like P_3 unit. The central P atom (P^A) of the P_3X_3 subunit resonates at low field (380 ppm for **2** and 421 ppm for **7**), while the peripheral P atoms (P^O/$P^{O'}$) resonate at moderately higher field (5 ppm for **2** and 145 ppm for **7**) and show a smaller $^1J_{PP}$ coupling constant (~280 Hz; Figure 1b). Within the $PBrPBr_2$ unit of **5**, the $^1J_{PP}$ coupling of 420 Hz is rather large and an additional large coupling (J_{PAPH} = 70 Hz) is observed within the P_3 unit. Similarly, P–P couplings can be detected between the PCl_2 and the P_3 units (up to 35 Hz) in **8** (Figure 1c) and **10** (up to 41 Hz, Figure 3, bottom). Additionally, the resonance signal of the PCl_6^- anion in **8** is observed at −296 ppm in the ^{31}P NMR spectrum. Compound **8** shows rather broad signals at room temperature, which sharpen by lowering the temperature to −40 °C (Figure 1c).

The $^{31}P\{^1H\}$ NMR spectrum of **6** shows two doublets with a coupling constant of 38 Hz, corresponding to the two non-equivalent phosphorus atoms. The signal at the highest field can be assigned to the PH ligand which splits in the ^{31}P NMR spectrum into a doublet due to the coupling with the proton ($^1J_{PH}$ = 444 Hz). For **9**, only one singlet was detected (cf. Supporting Information). The ^{31}P NMR chemical shifts and coupling constants for all complexes were determined by iterative simulation of the experimental spectra (see Supporting Information).

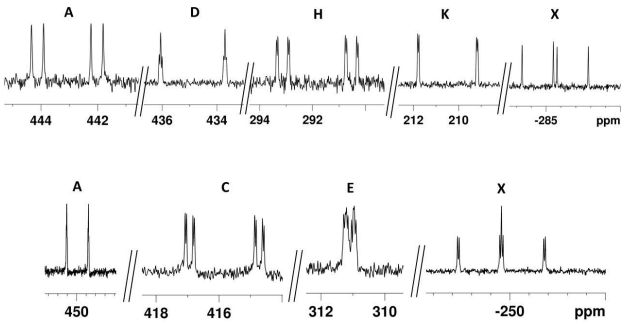

Figure 3. Selected signals of the $^{31}P\{^1H\}$ NMR spectra of **5** (top) and **10** (bottom) (CD_2Cl_2, 300 K).

Apart from **7** which is extremely unstable even at low temperatures in solution and could not be isolated, the solid-state structures of all other products were determined by single crystal X-ray diffraction analysis (Figure 4), revealing that the halogenation of the 28VE *cyclo*-P_6-containing triple-decker complex $[(Cp^*Mo)_2(\mu,\eta^6{:}\eta^6\text{-}P_6)]$ (**1**) leads to the formation of dinuclear monocations and neutral species which, in most cases, retain their triple-decker geometry. However, in some cases, degradation to $[(Cp^*MoBr_2)_2(\mu\text{-}Br)_2]$, $[(Cp^*Mo)(I_4)]^-$ or $[Cp^*MoX_4]$, the latter being observed as an anion in **4** and **11**, was detected. For all complexes, the Mo–Mo bond lengths are below the sum of their covalent radii (3.08 Å)[22] and longer than the corresponding distance in the neutral *cyclo*-P_6 complex **1** (2.647(1) Å)[13] and in the related monocation $[(Cp^*Mo)_2(\mu,\eta^6{:}\eta^6\text{-}P_6)][FAl]$ ($[FAl] = [FAl\{OC_6F_{10}(C_6F_5)\}_3]$, 2.661(8) Å).[14] They vary from 2.691(2) Å in **9** to 2.920(6) Å in **10**. The only exception is observed within **4** with a Mo–Mo distance of 2.579(6) Å. The Cp* ligands in the compounds **2-I$_3$**, **3**, **4**, **6**, **8**, **9** and **11** are almost coplanar to each other, being only minimally tilted (tilt angle of 1° to 7°). In compounds **5** and **10**, the coplanarity of the ligands is lost, and the Cp* ligands are tilted by 40° and 38°, respectively.

The molecular structure of **2-I$_3$** shows an allylic-P_3 and a P_3I_3 ligand each of them bridging the two {Cp*Mo} fragments (Figure 4). In the P_3I_3 unit, the central P atom does not coordinate to molybdenum. Compared to the P–P bond lengths in **1**[13] (average: 2.171(3) Å and in the range of P–P single bonds (2.22 Å)[23]), the P3-P4 (2.139(5) Å) and P4-P5 (2.138(6) Å) distances are shortened. Similar bond lengths were observed for the cationic complex $[(Cp^*Mo)_2(\mu,\eta^6{:}\eta^6\text{-}P_6)][FAl]$[14] whose *cyclo*-$P_6$ undergoes a bis-allylic distortion upon one electron oxidation (average: 2.136(10) Å). The P1-P2 (2.216(5) Å) and the P1-P6 (2.220(5) Å) distances in the P_3I_3 ligand are longer than the one in **1**, and correspond to P–P single bonds, while the distance between P2 and P6 with 2.459(5) Å is too long for a usual single bond, but considerably below the sum of the van der Waals radii (3.80 Å).[22] DFT calculations for compound **2-I$_3$** reproduce this distance (2.434 Å) well, but no bonding interaction could be detected between these two P atoms (the Mayer bond order (BO) is lower than 0.1 and no orbital overlap occurs). The P···P distances between the two P_3 ligands are rather long (P2···P3 2.652(5) Å and P5···P6 2.665(5) Å). Nevertheless, DFT calculations indicate the presence of a P···P interaction as shown by BOs of 0.16 and 0.18 for P2···P3 and P5···P6, respectively (see also Supporting Information). A similar *cyclo*-P_3I_3 moiety was recently postulated by DFT computations as one of the intermediates involved in the last steps of the iodine-induced stepwise degradation of the P_4 ligand in $[Cp^*Ru(dppe)(\eta^1\text{-}P_4)]$,[7] but without any experimental evidence. Therefore, **2-I$_3$** represents the first example of an isolated polyphosphorus complex bearing a P_3I_3 ligand. The presence of an allylic P_3 ligand is recurrent among the products of the halogenation of **1**, as in **4**, **5**, **8** and **10**, which will be discussed together therefore. In the allylic P_3 ligand of **4**, the P1–P2 (2.126(2) Å) and the P2-P3 (2.118(19) Å) bond lengths are shortened compared to the P–P

Research Article
doi.org/10.1002/chem.202200669

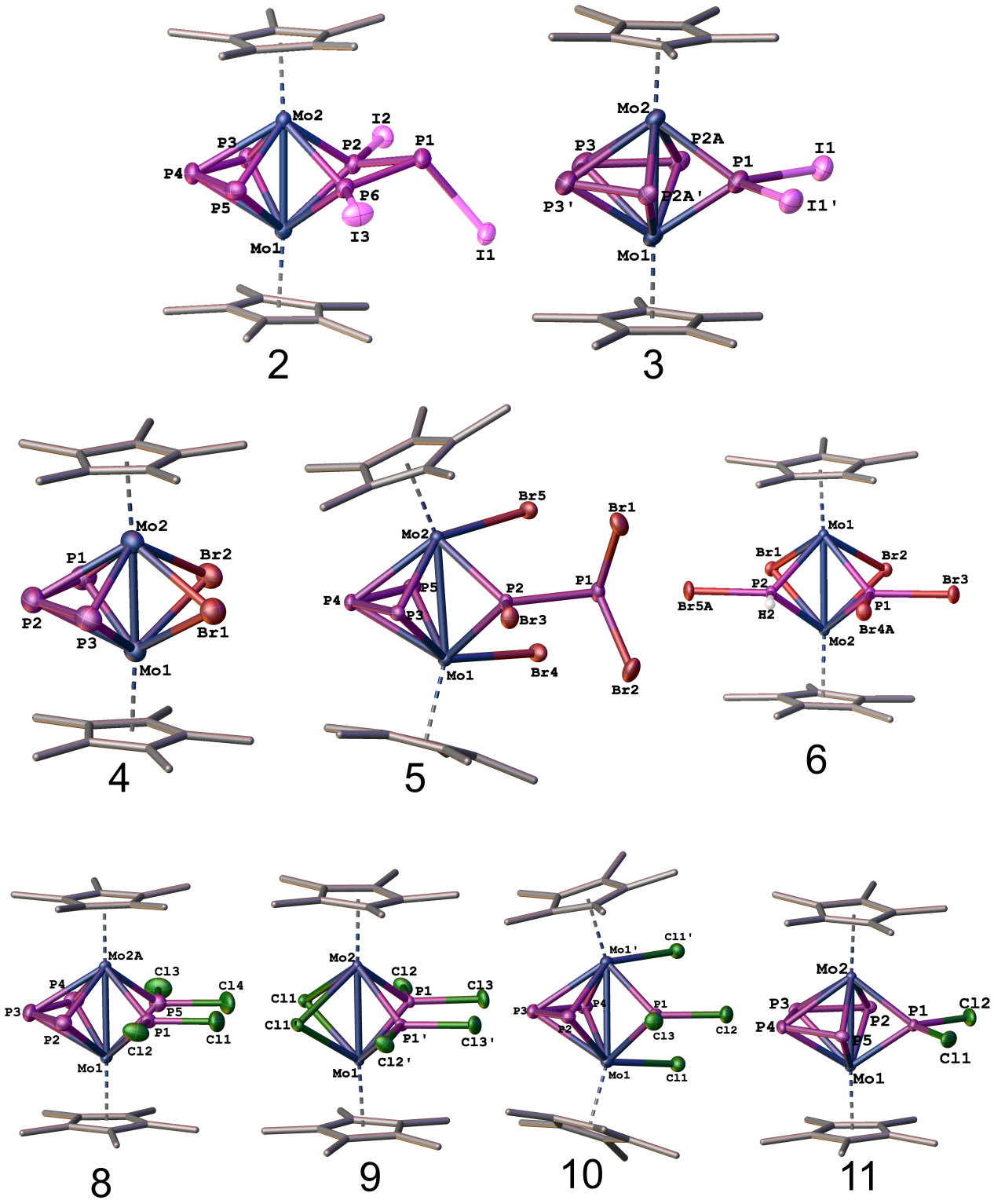

Figure 4. Molecular structures of **2-I$_3$**, **3**, **4**, **5**, **6**, **8**, **9**, **10** and **11** with thermal ellipsoids at 50% probability level. Hydrogen atoms and the counterions of **2-I$_3$**, **3**, **4**, **8** and **11** are omitted for clarity. In case of disorder only the major parts are depicted. Selected bond lengths: **2I$_3$**: Mo1–Mo2: 2.722(15) Å, P1–P2: 2.216(5) Å, P1–P6: 2.220(5) Å, P3–P4: 2.139(5), P4–P5: 2.138(6) Å; **3**: Mo1–Mo2: 2.743(8) Å, P2A–P3A: 2.243(7) Å, P3–P3′: 2.162(4); **4**: Mo1–Mo2: 2.579(6) Å, P1–P2: 2.126(2) Å, P2–P3: 2.118(19) Å; **5**: Mo1–Mo2: 2.919(7) Å, P1–P2: 2.260(2) Å, P3–P4: 2.174(2) Å, P4–P5: 2.128(2) Å; **6**: Mo1–Mo2: 2.709(3) Å; **8**: Mo1–Mo2: 2.728(2) Å, P2–P3: 2.105(4) Å, P3–P4: 2.101(4) Å; **9**: Mo1–Mo2: 2.691(2) Å; **10**: Mo1–Mo1′: 2.920 (6) Å, P2–P3: 2.163 (2) Å, P3–P4 2.123 (3) Å; **11**: Mo1–Mo2: 2.759(4) Å, P2–P3: 2.210(9) Å, P4–P5: 2.197(8), P3–P4: 2.155(9) Å.

bond lengths in **1** (average: 2.171(3) Å). In the case of **5**, the P_3 ligand is distorted (P3-P4 2.174(2) Å; P4-P5 2.128(2) Å) and additionally a P_2Br_3 ligand bridges the two {Cp*MoBr} fragments in an *end-on* coordination mode with a P–P bond length that is in the range of a P–P single bond (P1–P2 = 2.260(2) Å). Several diphosphines of the type RP_2Br_3 were reported, for example with R = ^{t}Bu by *Baudler* et al.,[24] R = CCl_3[25] or R = CN,[26] but no P_2Br_3 unit as a ligand attached to a metal fragment is known. Thus, the one in **5** is the first reported example. The P_3 ligand in **8** is in line with what was observed for the analog P_3 units in **2-I$_3$**, **4** and **5**, with P2-P3 = 2.105(4) Å and P3-P4 = 2.101(4) Å. The average distance from this unit and the PCl_2 groups (2.663(7) Å) suggests the presence of P···P interactions between them. The solid-state structure of **10** resembles the one observed for **5**, containing a distorted allylic P_3 ligand (P2-P3: 2.163(2) Å and P3-P4: 2.123(2) Å) bridging between two {Cp*MoCl} units. The short distance between the P_3 ligand and the PCl_2 group (P1-P2 = 2.577(19) Å) indicates an interaction which is also reflected in a rather large $^2J_{PP}$ coupling constant between these nuclei. The short P1···P2 distance (2.551 Å) is well reproduced by DFT calculations and is accompanied by a BO of 0.22 indicating the presence of a bonding interaction. The P_n core of **10** is similar to the one observed in compound [{Cp*V}$_2$(μ,η^3:η^3-P_3){μ-P-(NHC^{Me})}] resulting from the ring contraction of the vanadium analog of **1** ([(Cp*V)$_2$(μ,η^6:η^6-P_6)]) induced by ^{Me}NHC.[27]

The solid-state structure of **3** reveals a *cisoid*-P_4 and a PI_2 bridging ligand separated from each other by 2.596(9) Å. The P2-P3 (= P2′-P3′) (2.243(7) Å) and P3-P3′ (2.162(4) Å) bond lengths in the *cisoid*-P_4 ligand all lie in the range of P–P single bonds. Therefore, it cannot be described as a tetraphosphabuta-1,3-diene-like ligand, contrary to the analog *cisoid*-P_4 ligands in complexes [(Cp^{BIG}Fe)$_2$(μ,η^4:η^4-P_4)],[28] [(Cp′′Fe)$_2$(μ,η^4:η^4-P_4)],[29] [{Cp^{R}Fe}$_2$(μ,η^4:η^4-P_4)] (Cp^R = $C_5H_3(SiMe_3)_2$).[30] The *cisoid*-P_4 ligand as middle deck in the 30VE species **11** is similar to the one in **3** with two longer P–P bonds (P2–P3 = 2.210(9) Å, P4–P5 = 2.197(8) Å) and a shorter one (P3–P4 = 2.155(9) Å). The P1–P2 and the P1–P5 distances in **11** are 2.664(8 Å) and 2.6591(7), respectively, indicating a P–P interaction (see below).

The solid-state structure of **6** contains only two P atoms, in the form of a PBr_2 and a PHBr bridging ligand, with a nonbonding distance between the two phosphorus atoms of 2.762(9) Å. A similar structure was observed for compound **9**, which bears two equivalent bridging PCl_2 ligands, separated from each other by 2.894(6) Å.

In order to investigate the bonding situation in complexes **2**–**12**, DFT calculations at the D4-TPSSh(CPCM)/def2-TZVP level were conducted.[31] The geometric parameters of the complexes are well reproduced, including the distances between the different P_n units in the molecules. In all complexes **2**–**12**, a Mo–Mo bond was detected, being in line with the relatively short Mo–Mo distances. The Mayer bond order (BO) varies from 0.87 in **4** to 0.59 in **5** (Mo–Mo distances 2.574 and 2.892 Å in the optimized geometries, respectively). The intrinsic bonding orbitals[32] representing the Mo–Mo bond in **2** and the bonding within the Mo_2P_3 unit in **4** are depicted in Figure 5.

The NBO[33] analysis is in agreement with the IBO analysis, although only in **4** and **6** an Mo–Mo bond (Mo–Mo 2.579 Å (**4**) and 2.709 (**6**)) is predicted by the NBO analysis, while in the other complexes a nonbonding NBO on each Mo with an occupancy of approx. 1e is partitioned instead of a Mo–Mo bonding orbital. Although the P2–P6 distance in **2** is rather short, no bonding interaction could be detected by DFT calculations. In contrast, bonding interactions were detected between P2–P3 (2.649 Å) and P5-P6 (2.628 Å) as shown by BOs of 0.16 and 0.18, respectively. Similar interactions were detected between P1–P2 A in **3** (P1-P2 A 2.623 Å, BO 0.17; singlet spin state), P2–P3 in **5** (2.594 Å, BO 0.17), P1–P2 in **8** (2.517 Å, BO 0.24), P1–P2 in **10** (2.551 Å, BO 0.22), P2–P3 in **11** (2,626 Å, BO 0.18; singlet spin state) and P2–P3 in **12** (2.665, BO 0.17). The Interaction Region Indicator (IRI)[34] clearly shows a bonding interaction between the P_3 and the PCl_2 units in **8**, among the expected bonds. A plot of IRI in the plane defined by the phosphorus atoms is depicted in Figure 5 showing the regions with notable chemical bond interaction (orange) and areas where weak interactions occur (green). The Electron Localization Function (ELF)[35] and Localized Orbital Locator (LOL)[36] also support these interactions (see Supporting Information). Complexes **3** and **11** are paramagnetic in solutions at room temperature, however, DFT calculations show that the singlet spin state of the cation in **3** and **11** is with 90 and 102 kJ·mol^{-1}, respectively, more stable than the triplet spin state. The overall paramagnetic behavior of **11** might be due to the paramagnetic nature of the counter anions [Cp*MoCl$_4$]$^-$, having a triplet spin state as determined experimentally.[37]

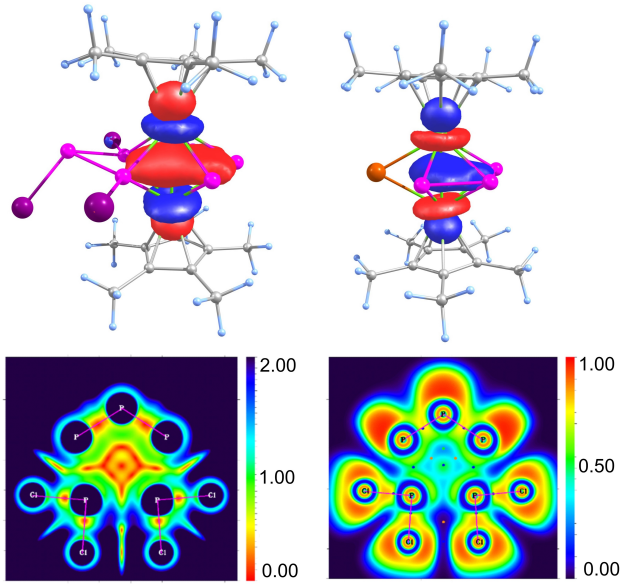

Figure 5. Intrinsic bonding orbitals representing the Mo–Mo bond in **2** (top left) and **4** (top right) as well as the Interaction Region Indicator (IRI) plot in the plane defined by the phosphorus atoms (bottom left) and Electron Localization Function (ELF) plot (bottom right) in **8**. Blue dots represent (3,−1) critical points.

Conclusions

In summary, we showed that the halogenation of $[(Cp^*Mo)_2(\mu,\eta^6{:}\eta^6\text{-}P_6)]$ (**1**) proceeds via a very complex pathway leading to a plethora of complexes containing different P_n units such as P_4, P_3, P_2 and P_1. An excess of halogens/halogen sources leads to phosphorus-free complexes of the type $[Cp^*MoX_n]$ (X = I, Br, Cl) as well as PX_3 (X = Br, Cl) as final reaction products. Additionally, we showed that besides iodination, which is known to be a powerful tool for the synthesis of new P_n ligand complexes, bromination and chlorination can also be used for this purpose. Among the products of the iodination of the hexaphosphabenzene complex **1**, the novel compound **2** bearing an unprecedented P_3I_3 ligand could be isolated. With a bromine source, complex **5** could be isolated, representing the first example of a compound bearing a P_2Br_3 unit as a bridging ligand between two Mo centers.

Whereas the products of the one-electron oxidation of **1** showed only a distortion of the hexagonal geometry of the P_6 middle deck, the use of halogens or halogen sources as oxidizing agents afforded a variety of new polyphosphorus compounds bearing synthetically useful novel P_nX_m units. As expected, the chemoselectivity of the reaction decreased with the enhancement of the oxidizing power of the halogen. However, with a strict control of the temperature it is possible to exert a good control of the reaction even with a stronger oxidant such as the chlorine source PCl_5. First snapshots from the halogenation of the P_6 ligand complex were found, and even though the complete pathway could not be clarified, they gave useful information concerning the progress of the reaction. Thus, first an allylic fragmentation of the *cyclo*-P_6 unit occurs followed by the monohalogenation of the P atoms of one of the allylic P_3 units. Subsequently, a dihalogenation forming PX_2 units occurs, which is followed by the removal of the P atoms as PX_3 moieties. Only afterwards, the second allylic-P_3 unit appears to be halogenated.

This study adds triple-decker complexes to the class of polyphosphorus compounds that can be successfully halogenated and thus functionalized. Therefore, future investigations will focus on the halogenation of heterobimetallic triple-decker compounds as well as of E_n ligand derivatives that combine the features of triple-decker complexes and separate E_n units. Moreover, since the halogenation reactions in general have shown to be a powerful tool for the generation of halogen-functionalized polyphosphorus ligands, future studies will also focus on the use of these products for further derivatizations.

Deposition Numbers 2155218 (**2-I$_3$**), 2155219 (**3**), 2155220 (**4**), 2155221 (**5**), 215522 (**6**), 2155223 (**8**), 2155224 (**9**), 2155225 (**10**) 2155226 (**11**) and 2155227 (**12**) contain the supplementary crystallographic data for this paper. These data are provided free of charge by the joint Cambridge Crystallographic Data Centre and Fachinformationszentrum Karlsruhe Access Structures service.

Acknowledgements

The Deutsche Forschungsgemeinschaft (DFG) is gratefully acknowledged for the support within the project Sche384/36-2. Open Access funding enabled and organized by Projekt DEAL.

Conflict of Interest

The authors declare no conflict of interest.

Data Availability Statement

The data that support the findings of this study are available in the supplementary material of this article.

Keywords: bromine · chlorine · halogenation · hexaphosphabenzene · iodine · phosphorus

[1] J. A. Besson, *Compt. Rend.* **1897**, *124*, 1346–1349.
[2] R. Bouloch, *Compt. Rend.* **1905**, *141*, 256.
[3] D. Wyllie, M. Ritchie, E. B. Ludlom *J. Chem. Soc.* **1940**, 583–587.
[4] B. W. Tattershall, N. L. Kendall *Polyhedron* **1994**, *13*, 1517–1521.
[5] P. Barbaro, C. Bazzicalupi, M. Peruzzini, S. Seniori Costantini, P. Stoppioni, *Angew. Chem. Int. Ed.* **2012**, *51*, 8628–8631.
[6] M. Bispinghoff, Z. Benkő, H. Grützmacher, F. Delgado Calvo, M. Caporali, M. Peruzzini, *Dalton Trans.* **2019**, *48*, 3593–3600.
[7] G. Manca, A. Ienco, *Inorg. Chim. Acta* **2021**, *517*, 120205.
[8] C. Mealli, A. Ienco, M. Peruzzini, G. Manca, *Dalton Trans.* **2018**, *47*.
[9] H. Brake, E. Peresypkina, A. V. Virovets, M. Piesch, W. Kremer, L. Zimmermann, Ch. Klimas, M. Scheer, *Angew. Chem. Int. Ed.* **2020**, *59*, 59, 16241–16246.
[10] A. Garbagnati, M. Seidl, G. Balázs, M. Scheer, *Inorg. Chem.* **2021**, *60*, 5163–5171.
[11] L. Dütsch, M. Fleischmann, S. Welsch, G. Balázs, M. Scheer, *Angew. Chem. Int. Ed.* **2018**, *57*, 3256–3261.
[12] M. V. Butovskiy, G. Balázs, M. Bodensteiner, E. V. Peresypkina, A. V. Virovets, J. Sutter, M. Scheer, *Angew. Chem. Int. Ed.* **2013**, *52*, 2972–2976.
[13] O. J. Scherer, H. Sitzmann, G. Wolmershäuser, *Angew. Chem.* **1985**, *97*, 358–359; *Angew. Chem. Int. Ed. Engl.* **1985**, *24*, 351–353.
[14] M. Fleischmann, F. Dielmann, G. Balázs, M. Scheer, *Chem. Eur. J.* **2016**, *22*, 15248–15251.
[15] J. C. Gordon, V. T. Lee, R. Poli, *Inorg. Chem.* **1993**, *32*, 4460–4463.
[16] J. U. Desai, J. C. Gordon, H. Kraatz, V. T. Lee, B. E. Waltermire, R. Poli, A. L. Rheingold, C. B. White, *Inorg. Chem.* **1994**, *33*, 3752–3769.
[17] In the ^{31}P NMR spectrum of the reaction solution, only one of the two signals of **4** could be detected, probably due to its low concentration, whereas the characteristic signal of its counterion $[Cp^*MoBr_4]^-$ could be detected in the ^{1}H NMR spectrum.
[18] Determined by ^{31}P NMR spectroscopy (cf. Supporting Information).
[19] H. B. Kraatz, R. Poli, *J. Organomet. Chem.* **1994**, *475*, 167–175.
[20] Unfortunately, complex **12** could be obtained only once. All attempts to synthesize **12** in a targeted manner have failed so far.
[21] The use of a smaller number of equivalents of PCl_5 (1, 2 or 3 equiv.) did not lead to an improvement of the chemoselectivity and often resulted in the crystallization of the residual **1**, even though it was not detected in the ^{31}P NMR spectrum. The use of a large excess of the halogenating agent (10 equiv.) led e.g. to the isolation of the known compound $[(Cp^*MoCl)_2(\mu\text{-}Cl)_2]$ in 14% crystalline yield, see Ref. [37].
[22] S. Alvarez, *Dalton Trans.* **2013**, *42*, 8617–8636 .
[23] P. Pyykkö, M. Atsumi, *Chem. Eur. J.* **2009**, *15*, 12770–12779.
[24] M. Baudler, J. Hellmann, *Z. Anorg. Allg. Chem.* **1982**, *490*, 11–18.
[25] P. L. Airey, *Z. Naturforsch.* **1969**, *24b*, 1393–1397.
[26] K. B. Dillon, A. W. G. Platt, T. C. Waddington, *Inorg. Nucl. Chem. Lett.* **1981**, *17*, 201–205.
[27] M. Piesch, S. Reichl, M. Seidl, G. Balázs, M. Scheer, *Angew. Chem. Int. Ed.* **2019**, *58*, 16563–16568.

[28] S. Heinl, G. Balázs, M. Scheer, *Phosphorus, Sulfur, and Silicon and the Related Elements*, *189*, **2014**, 1–9.
[29] O. J. Scherer, G. Schwarz, G. Wolmershäuser, *Z. Anorg. Allg. Chem.* **1996**, *622*, 951–957.
[30] V. A. Miluykov, O. G. Sinyashin, P. Lonnecke, E. Hey-Hawkins, *Mendeleev Commun.* **2003**, *13*, 212–213.
[31] D4-TPSSh(CPCM)/def2-TZVP level: a) D4: E. Caldeweyher, S. Ehlert, A. Hansen, H. Neugebauer, S. Spicher, C. Bannwarth, S. Grimme, *J. Chem. Phys.* **2019**, *150*, 154122; b) TPSSh: J. Tao, J. P. Perdew, V. N. Staroverov, G. E. Scuseria, *Phys. Rev. Lett.* **2003**, *91*, 146401; c) V. N. Staroverov, G. E. Scuseria, J. Tao, J. P. Perdew, *J. Chem. Phys.* **2003**, *119*, 12129–12137; d) Erratum: *J. Chem. Phys.* **2004**, *121*, 11507–11507; e) CPCM: J. Tomasi, B. Mennucci, R. Cammi, *Chem. Rev.* **2005**, *105*, 2999–3094; f) def2-TZVP: F. Weigend, R. Ahlrichs, *Phys. Chem. Chem. Phys.* **2005**, *7*, 3297–3305.
[32] G. Knizia, *J. Chem. Theory Comput.* **2013**, *9*, 4834–4843.
[33] NBO 6.0. E. D. Glendening, J. K. Badenhoop, A. E. Reed, J. E. Carpenter, J. A. Bohmann, C. M. Morales, C. R. Landis, F. Weinhold (Theoretical Chemistry Institute, University of Wisconsin, Madison, WI, 2013); http://nbo6.chem.wisc.edu/.
[34] T. Lu, Q. Chen, *Chemistry–Methods* **2021**, *1*, 231–239.
[35] a) C. F.-W. L. Tian, *Acta Phys. Chim. Sin.* **2011**, *27*, 2786–2792; b) A. Savin, O. Jepsen, J. Flad, O. K. Andersen, H. Preuss, H. G. von Schnering, *Angew. Chem. Int. Ed. Engl.* **1992**, *31*, 187–188; c) A. D. Becke, K. E. Edgecombe, *J. Chem. Phys.* **1990**, *92*, 5397–5403.
[36] H. Jacobsen, *Can. J. Chem.* **2008**, *86*, 695–702.
[37] F. Abugideiri, G. A. Brewer, J. U. Desai, J. C. Gordon, R. Poli, *Inorg. Chem.* **1994**, *33*, 3745–3751.

Manuscript received: March 2, 2022
Accepted manuscript online: March 29, 2022
Version of record online: April 21, 2022